applied sciences

MDPI

Article

Impact of the Speed of Airflow in a Cleanroom on the Degree of Air Pollution

Pavol Mičko [1,*], Dávid Hečko [1], Andrej Kapjor [2], Radovan Nosek [2], Zuzana Kolková [1], Peter Hrabovský [1] and Nikola Čajová Kantová [1]

[1] Research Centre, University of Zilina, Univerzitna 1, 01026 Zilina, Slovakia; hecko@uniza.sk (D.H.); zuzana.kolkova@uniza.sk (Z.K.); peter.hrabovsky@uniza.sk (P.H.); nikola.cajovakantova@uniza.sk (N.Č.K.)

[2] Department of Power Engineering, Faculty of Mechanical Engineering, University of Zilina, Univerzitna 1, 01026 Zilina, Slovakia; andrej.kapjor@fstroj.uniza.sk (A.K.); radovan.nosek@fstroj.uniza.sk (R.N.)

* Correspondence: micko@uniza.sk; Tel.: +421-41-513-7620

Abstract: The high-energy requirements of cleanrooms are the main motivation for optimizing their operational conditions. The ventilation system consumes the most energy in order to ensure the precise air conditioning of the room (filtration, temperature, and humidity adjustment). The main function of the ventilation system is to keep particle concentration to a minimum. This work deals with the optimization of an experimental operating room via the optimization of air supply through the distribution element (laminar airflow ceiling) in the range of 0.15–0.25 $m \cdot s^{-1}$. The laminar airflow between the distribution element and the patient is influenced by the operating light and different airflow velocities. These factors affect changes in particle concentration. Ansys Fluent software was used to investigate the nature of the flow, velocity profiles, and particle trajectories. The results of our numerical simulation demonstrate that a suitable flow rate setting increases the efficiency of particle reduction in the operating table area by up to 54%, which can, in turn, reduce operating costs. The simulated air velocity profile was subsequently verified using the particle image velocimetry (PIV) method. The typical size of particles monitored for in cleanrooms is 0.5 µm according to ISO EN 7. Therefore, the results of this study should be helpful in correctly designing distribution elements for clean rooms.

Keywords: cleanroom; operating room; airborne particles; ventilation; airflow velocity; particle concentration

check for updates

Citation: Mičko, P.; Hečko, D.; Kapjor, A.; Nosek, R.; Kolková, Z.; Hrabovský, P.; Kantová, N.Č. Impact of the Speed of Airflow in a Cleanroom on the Degree of Air Pollution. *Appl. Sci.* **2022**, *12*, 2466. https://doi.org/10.3390/app12052466

Academic Editor: Min-Suk Bae

Received: 28 December 2021
Accepted: 24 February 2022
Published: 26 February 2022

1. Introduction

Cleanrooms are defined as areas with a low concentration of airborne particles. It is necessary to ensure their proper function for healthcare or precision manufacturing. A high concentration of airborne particles can affect product quality and functionality. These particles transport viruses, bacteria, and increase the risk of contamination during surgery in the operating room. The key principle of keeping a low concentration of particles is to supply a large amount of filtered air and thus reduce the particle concentration in the ventilated room to the required level [1]. Forced ventilation systems have high-performance requirements, as they control not only the transportation and filtration of air into a ventilated room, but also adjust the temperature and humidity of this air, resulting in a high amount of energy consumed for their operation [2–5]. Depending on the cleanroom classification, a clean zone's entire air volume must be replaced from once every 3 min (ISO EN 8) up to once every 10 s (ISO EN 4-1) [6]. According to studies [7,8], clean rooms consume 50–70% of the electricity supplied for HVAC (Heating, Ventilation, and Air Conditioning) systems in order to function properly. A survey conducted in Taiwan demonstrates the use of high-tech HVAC systems, which only consumes approximately 35% of electricity by using clean air recirculation. This value represents about 7.4% of total energy consumption [9].

Our objective is to reduce the operating cost of these energy-intensive systems while maintaining the required quality of the cleanroom's internal environment (low concentration of particles in the air). As the industry develops, enforcing progressively stricter requirements for environmental cleanliness in the operation of medical and pharmaceutical facilities, the fiscal advantages that come with the appropriate modification of HVAC systems grow ever larger [5]. This approach also contributes to sustainable business. Since the 20th century, many studies and scientific articles have focused intensively on reducing the energy requirements of clean rooms. The air change rates (ACH) value, the location of the inlet/outlet, the source of contaminants, as well as the influence of external factors in airflow distribution and air quality were monitored [10–15]. Several research studies have identified various barriers to energy efficiency in cleanrooms and have suggested options to improve energy efficiency [16–18].

One of these options is to optimize airflow and its regulation by improving the energy efficiency of the ventilation system [19]. For example, reducing the energy cost of fan power by 33% would contribute to a 66% reduction in energy consumption [20]. Previous studies have shown that demand-controlled filtration can lead to annual energy savings ranging from 28% to 72% [21–24]. Another way to reduce the energy consumption of a cleanroom is to move the air supply and exhaust distribution elements closer to the source of the pollution and the clean zone of the ventilated space. This can reduce energy consumption by up to 20% while maintaining the required environmental quality. Using ventilation system circulation outside of the occupied space will reduce the energy consumption of fans by up to 70% [19]. However, this solution is not appropriate in several countries from a legislative point of view.

A cleanroom environment has many potential sources of contamination. These may vary depending on the number of people in the room, the purpose of the room, etc. However, the main sources of contamination are people, the material of their clothing, the room's structural elements, and the ventilation system itself, whose filters work with specified efficiency [25]. The actual rate of particle generation is often an unknown parameter when designing a cleanroom. As a result, HVAC systems are usually oversized to ensure compliance with the classification requirements [2,3,7,26]. Lenegan's study concluded that in some cases, the concentrations of particles were 10–100 times lower than the necessary parameters and that the rooms were of a higher purity class entirely [7]. According to Khoo et al. [2], the control of internal contaminants in cleanrooms with overpowered and oversized ventilation systems comes about because the designs and ACH values of these systems are based on principles published in a standard or code, such as the Federal Standard FS-209 [27], IEST Best Practices RP-12.1 [28], or ISO Std. 14644-4: 2004 [29].

The study by Khoo, et al. shows a direct connection between the reduction in the concentration of particles in a cleanroom, the increase in the ACH, and the share of the floor area for the extraction of polluted air. These results were obtained at 60–146 h^{-1} ACH, which are typical for high purity classes [2]. Heidrich et al. [30] stated that increasing the ventilation rate is the easiest way to improve air quality and cleanliness. However, studies on pollutant reduction have shown that high ACH values may not always guarantee a higher purity class, as shown by the studies of Zhao and Cheng [31]. They performed numerical and experimental investigations of the effects of ACH on airflow distribution and CO_2 concentration in a clean room with unidirectional airflow. The results illustrated that the recommended ACH should be based on room characteristics rather than empirical formulas. The increase of ACH from 15 h^{-1} to 20 h^{-1} did not significantly affect the pollutant removal efficiency in the occupied zone of a Class 10,000 cleanroom model. On the other hand, increasing the ACH from 20 h^{-1} to 25 h^{-1} showed a visible reduction in room residence time from 32% to 21% [32]. In contrast to the study by Zao et al. the study focused on the higher ACH range, 20–40 h^{-1}, typical of purity classes ISO EN 7–8, where most operating theaters are included. Various mathematical models have been proposed to represent the relationship between particle concentration in clean rooms and ACH, but some factors that could affect the accuracy of the model have not been considered to simplify them. Continuous generation of particles or their removal due to the operation of the ventilation system and settling of particles on the surface of the equipment and internal structures were not considered [33–36].

From the presented studies, one may conclude that there is a relationship between ACH and the value of the concentration of particles in the cleanroom. This assumption was verified in this study by using numerical simulations and experimental measurements to display the air velocity profile. The aim of this work was to determine the optimal airflow rate through the supply distribution element in the operating room. The main criteria for the optimal setting of air velocity and flow were to maintain a low concentration of particles in the patient area and amongst the instruments, a low energy consumption ventilation system, and to ensure the required temperature and humidity of the room.

2. Materials and Methods

This work examines the effect of laminar airflow ceiling (LAFC) over the operating zone. The study focuses mainly on decreasing the volume flow of the ventilation system, and reducing the operational costs and energy consumption of the cleanroom while maintaining the required concentration of particles or even their reduction. A computational fluid dynamics (CFD) model was created using ANSYS software (Fluent) to calculate air distribution and particle flow in the cleanroom. The same procedure for calculating the air distribution was used in the study released by Zao et al. [32]. The suitability of using CFD simulation is also reported by Villafruela et al. [37], which monitors the influence of the location, the types of distribution elements, and the source of pollution. Other studies had a similar intention regarding the performance of laminar airflow in the patient's operating room area [38–42]. Cheng et al. [43] used a numerical simulation to study the effects of the inlet velocity profile, room width, height, and the porosity of the raised floor on the uniformity of air velocity distribution in clean rooms with vertical direct flow. To verify the accuracy of the calculated airflow around the patient on the surgical table, the flow area between the operating light and the table will be analyzed in CFD models and compared to the experimental results performed using the PIV method.

2.1. CFD Simulation

In order to understand the mechanisms of particle movement, it is appropriate to use a CFD simulation to analyze the effects of airflow rates upon the total concentration of particles in the clean zone. An important part of this is to correctly set the boundary conditions of the simulation and the geometric conformity of the model with the actual geometry, for subsequent verification by the CFD simulation.

2.1.1. Model

The geometry of the model was developed in real dimensions, exactly preserving the dimensions of the interior equipment, such as the operating table, instrument tables, and the operating lamp. The model also includes six people as a source of heat and particles. The positions of the luminaire and the humans in the CFD simulation model is shown in Figure 1. The dimensions of the operating room model are $5.76 \times 6.05 \times 2.70$ m. The dimensions of the model and interior equipment copy the actual dimensions of the experimental laboratory in Figure 2.

The total air volume in the CFD model is divided into four parts. The first is VOT, which presents the volume of air above the operating table, where the floor plan dimensions copy the dimensions of the operating table, 2000×500 mm, with a height of 500 mm. The patient is included in this volume. The other two volumes, named VIT 1 and VIT 2, copy the floor plan dimensions of the instrument tables, 600×450 mm, and the height is 300 mm. These reference volumes are used to compare the number of particles inside the clean zone. They are proportional to the total amount of particles that are in the volume around the reference volumes. The resulting ratio of particles within the control volume and all particles in the room illustrates the improvement or deterioration of the environment's cleanliness for different operating conditions. The volumes are shown in the following Figure 3.

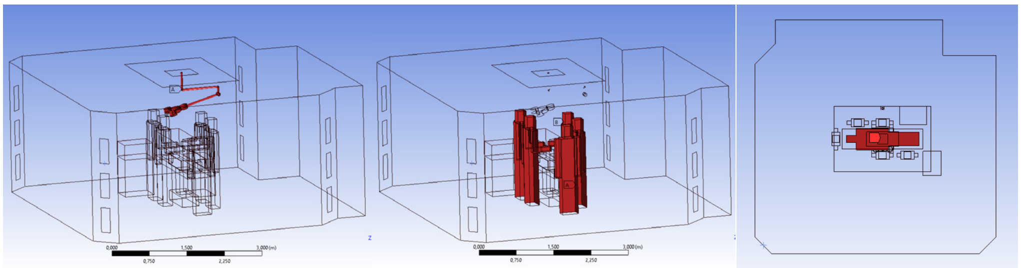

Figure 1. Position of the lamp, staff, and patient in the CFD simulation of the operating room.

Figure 2. Experimental clean room laboratory.

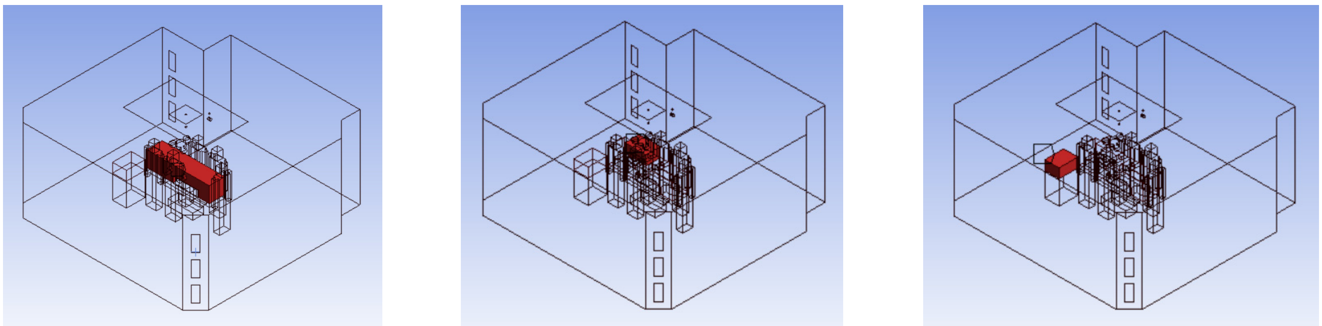

(**a**) (**b**) (**c**)

Figure 3. Reference volumes for monitoring the number of particles in the clean zone: (**a**) V_{OT}; (**b**) $V_{IT\,1}$; (**c**) $V_{IT\,2}$.

The filtered air was distributed to the room using a laminar field with dimensions 2400 × 1600 mm (Figure 4a). The air from the room was be discharged through the exhaust diffusers in the corners of the room (Figure 4b).

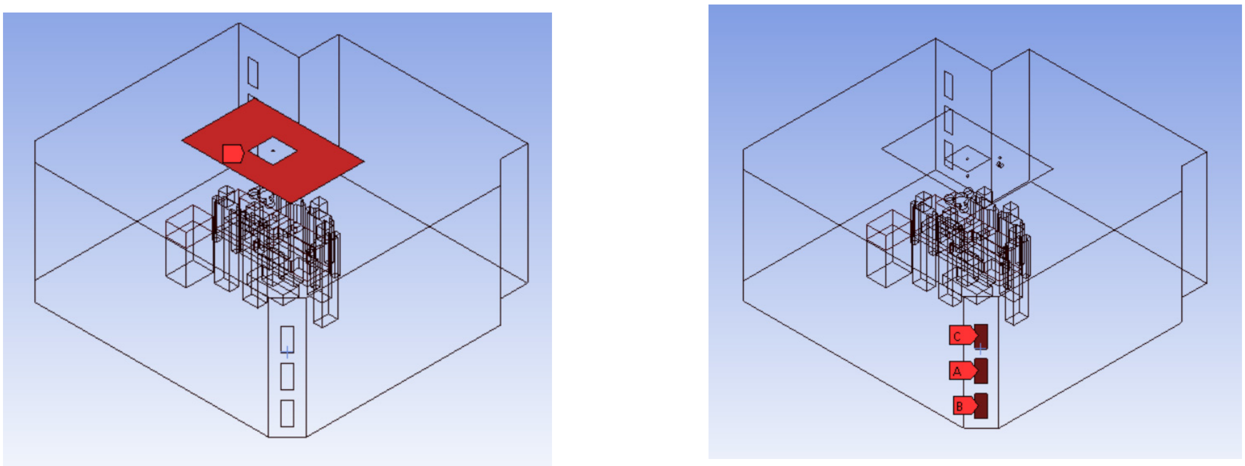

(**a**) (**b**)

Figure 4. Distribution elements (**a**) LAFC and (**b**) exhaust diffusers.

Several parameters affect the character of the particle flow in the operating room. The different states in the operating room can be projected by setting the simulation boundary conditions correctly. The mesh of the CFD model was densified around obstacles to filtered airflow trajectory in the room to capture unwanted turbulence and to faithful represent the Coanda effect as air flows around the objects. The greatest influence on airflow is the ceiling lamp located above the operating table. In addition to disturbing the directed flow, the air velocity profile may be affected by the higher surface temperature of the light source. The element type was subsequently modified using Ansys Fluent solution software to a polyhedra type in order to improve the quality of the network and reduce the number of elements. The simulation was performed in transient mode, so it was time dependent. The time step of one iteration was chosen to be 0.05 s and the total simulated time was 5 min. The gravity and energy model makes it possible to simulate buoyancy forces and the effect of natural convection caused by different temperature gradients. In this work, an energy-neutral environment without external heat loads or losses through the perimeter structures of the operating room is considered. Heat gains are only considered from the staff and the operating light. The temperature of structures, equipment, and air supply is 24 °C. The surface temperature of the operating LED lamp was set to 40 °C. A higher temperature, in combination with the Coanda effect, results in a change in the airflow velocity profile. The surface temperatures of the human body were set at 30 °C. Humans are the majority source of particles, as the natural convection caused by the temperature gradient from peoples' bodies can affect their distribution throughout the operating room. The multi-phase model ensures the emission of a given number of particles from each of the selected areas. According to measurements, one person in an ISO EN 7 cleanroom produces approximately 30,000 particles per minute up to 0.5 µm in size [44]. This value is calculated based upon the emission of particles from the surface of the body, clothing, talking, breathing, coughing, and other activities. The ventilation system is a mechanism for cleaning the building, but its filtering ability is not perfect. Although the (HEPA) filters serve to eliminate the measurement error by the primary particles [45], filters will miss a certain amount of particles, which was considered in the simulation at 25 min^{-1} in one cubic meter of supply air.

This exercise has proven that a higher amount of air flowing into the operating room does not necessarily mean a lower concentration of particles [31]. The increased airflow rate causes undesired turbulence around the barriers between the laminar field and the patient in the operating room. Thus, when designing a distribution laminar field for a clean room, a compromise is sought between maintaining the required airflow rate from the laminar field, maintaining a hygienic air exchange, and choosing a suitable size for the free outlet area of the laminar field. The recommended discharge velocities from a laminar field of 0.15–0.25 m·s^{-1} with a graduation of 0.025 m·s^{-1} are used in this simulation. The amount of air transported at different speeds is expressed by the continuity equation. The same amount of air is discharged from the operating zone and evenly distributed between the four corners of the room.

2.1.2. Results

The effects of the airflow rate upon the cleanliness of the room are expressed as the percentage of particles present in the reference volumes compared to the number of particles in the total volume. Figure 5 shows the following variations in the number of particles: in the volume above the operating table, V_{OT}, in the volume above the instrument table of the clean zone, $V_{IT\,1}$, and in the volume above the instrument table extending outside the clean zone, $V_{IT\,2}$. In addition to the contamination of the operating table, it is also essential to document the contamination of the instrument tables, due to the direct contact of the instruments with the patient's wound.

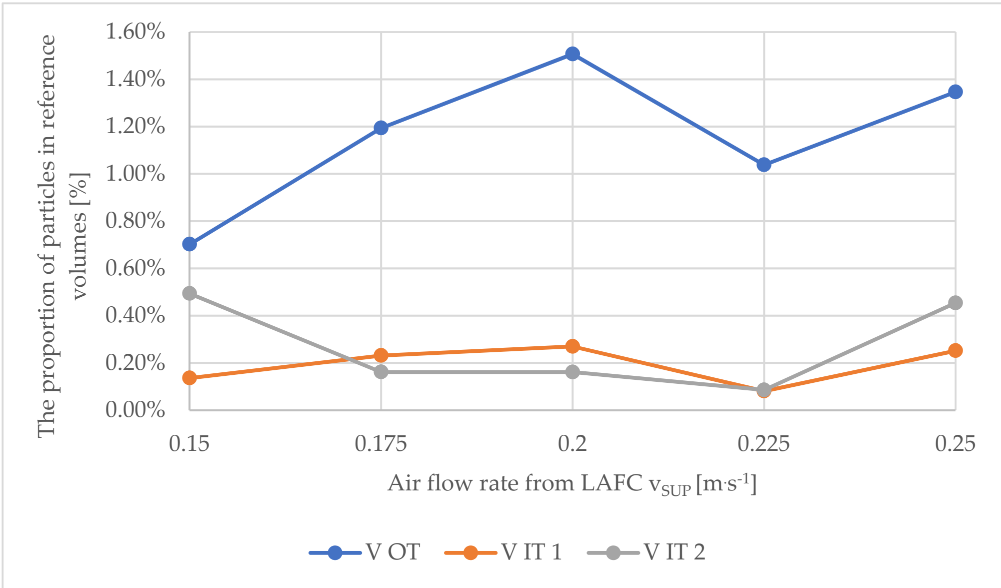

Figure 5. Percentage of particles in reference volumes depending on the airflow rate from LAFC.

Two imaging planes passing through the center of the model were created to show the air velocity profiles in the room (Figure 6). The air velocity profiles for the individual variants are shown in Figures 7–11.

Based on the presented results, we can evaluate the effects of air velocity from the distribution element on the concentration of particles in the cleanroom. The lowest number of particles in the reference volume found on the instrument tables were calculated for variants 2 to 4. A significant concentration increase can be observed in variant 5 when the air enters the reference volume at a velocity above 0.27 m·s^{-1}. The same phenomenon was observed in variant 1 for volume $V_{IT\,2}$ (instrumental stage extending outside the clear zone below the laminar field). As can be seen in Figure 12, a flow velocity above 0.27 m·s^{-1} is accumulated in the reference volume due to undesired turbulence caused by the airstream bouncing off the room's walls. Similarly, in the reference volume above the V_{OT} operating table, we observed an increase in the concentration of contaminants from the increased airflow rate through the LAFC. In evaluating the results of Figure 5 and from the airflow profiles in Figures 7–11, we can deduce two independent mechanisms affecting the removal of contaminants from the reference volume. The first mechanism works on the principle of diluting the concentration of contaminants by supplying filtered air. The more filtered air is introduced into the room, the lower the total concentration due to the removal of polluted air. The second mechanism of particle removal is to prevent the formation of unwanted turbulence in the area of reference volumes. As the amount of filtered air supplied increases with the use of the dilution mechanism, the flow rate through the LAFC increases (unless its type or size changes). A higher discharge velocity will cause an increase in the airflow rate even in the area of the reference volumes, which directly leads to a higher degree of turbulence. The increase in speed in the area of the reference volume "V_{OT}" can be seen especially on the imaging plane XY and YZ, wherein the area of the patient's torso and staff hands. The flow of particles through the reference volume can also be explained as the flow of particles through the path of least resistance since the flow of air in other directions is prevented by medical staff and the table. The task of the LAFC is to use a stabilized laminar airflow to create an imaginary piston that pushes all contaminants away from the patient. Thus, when the laminar flow is disturbed, contaminants penetrate the reference volume. For this reason, we consider it important to set the operating speed of the airflow through the LAFC correctly.

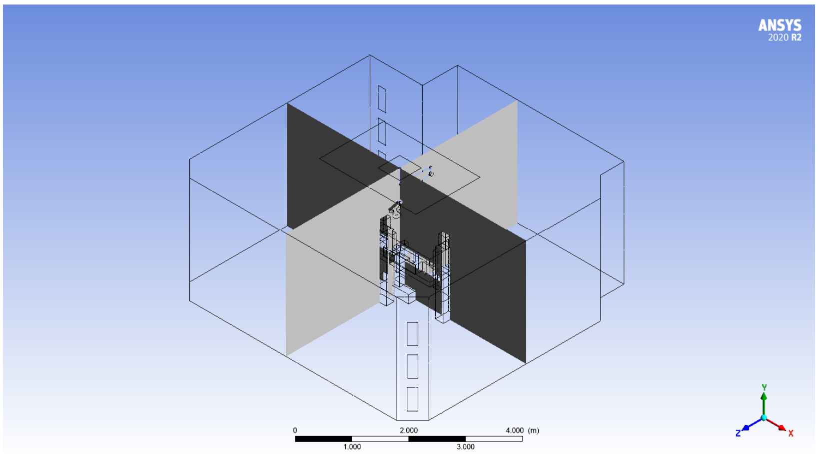

Figure 6. XY and YZ planes for displaying simulation outputs.

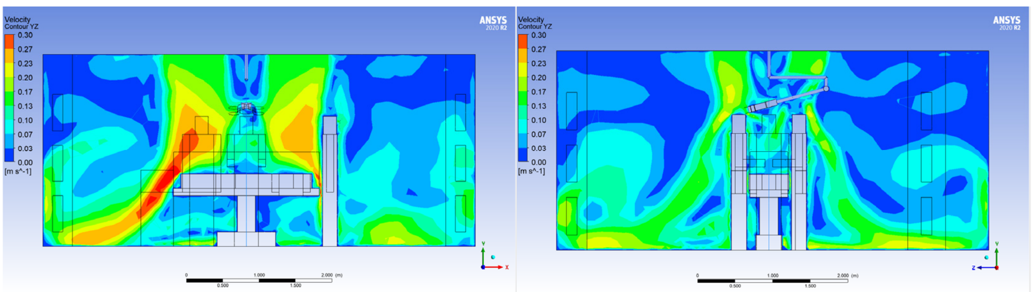

Figure 7. Air velocity profiles for variant 1 on the XY plane (**left**) and YZ (**right**).

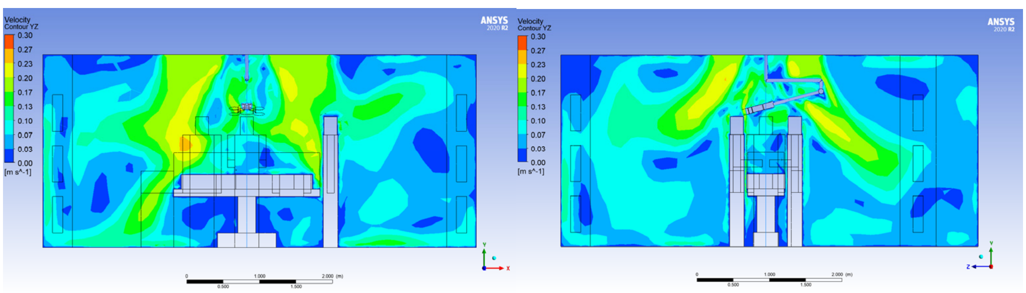

Figure 8. Air velocity profiles for variant 2 on the XY plane (**left**) and YZ (**right**).

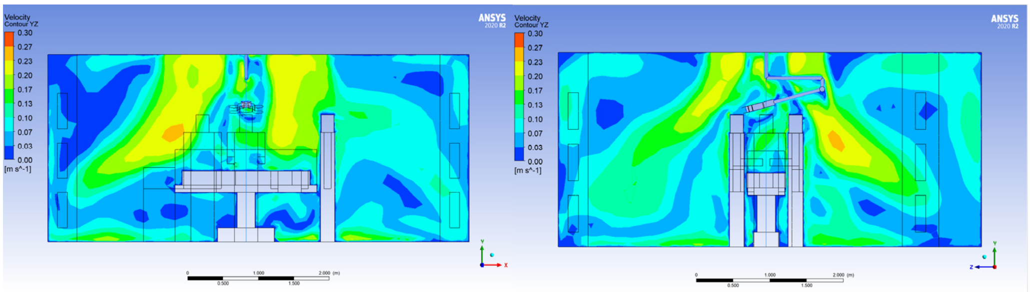

Figure 9. Air velocity profiles for variant 3 on the XY plane (**left**) and YZ (**right**).

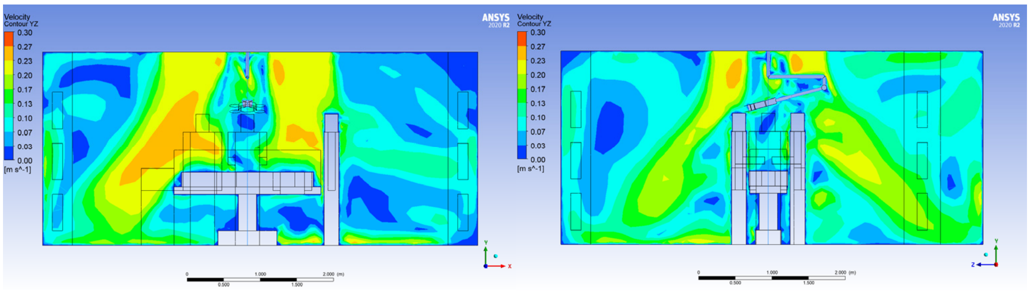

Figure 10. Air velocity profiles for variant 4 on the XY plane (**left**) and YZ (**right**).

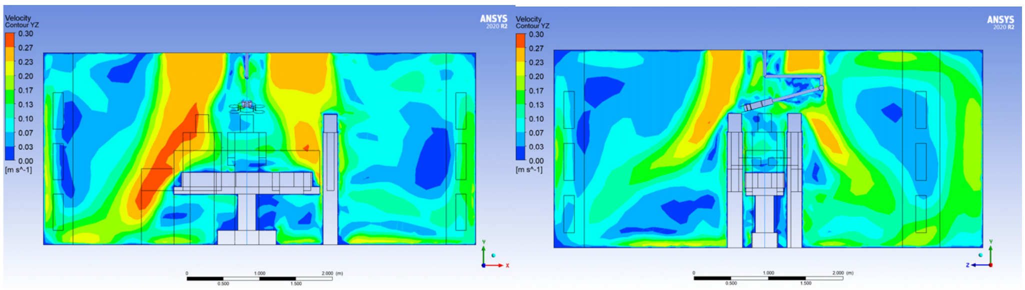

Figure 11. Air velocity profiles for variant 5 on the XY plane (**left**) and YZ (**right**).

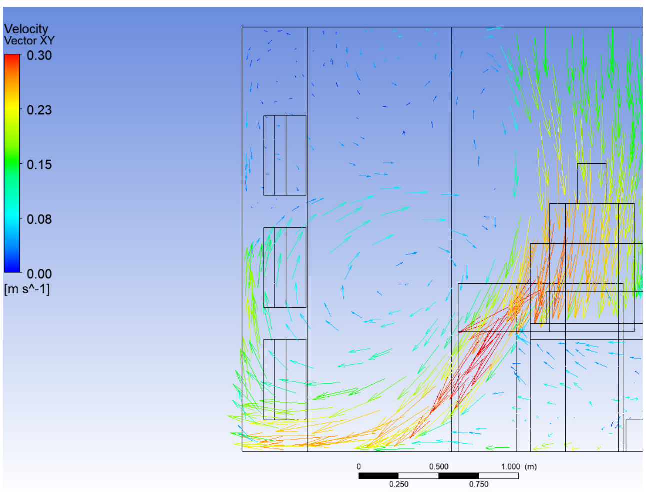

Figure 12. Air velocity vectors at $V_{IT\,2}$ reference volume.

2.2. Verification of Air Flow in CFD Simulation Using the PIV Method

The main mechanism of particle motion is forced convection formed by the ventilation system. The PIV (Particle Image Velocimetry) method was used to compare the CFD simulation with the experimental measurements. This is an immediate vector or scalar measurement of velocity in a cross section. The principle was to make a monitored plane using a pair of lasers with an adjustable switching frequency. The Dantec Dual PIV Laser creates a plane in which the movement of particles between individual switches is monitored. The inaccuracy of the PIV method measurement is determined by the maximum cross-correlation deviation of the two light pulses and the maximum value is up to 5%. The velocity vector tracking particles are delivered to the laminar field flow space using the Safex F2010 smoke generator, particle motion was recorded by a high FPS camera, and the devices used for scanning the speed profiles are shown in Figure 13.

(**a**) (**b**) (**c**)

Figure 13. Devices for scanning speed profiles using the PIV method: (**a**) Safex F2010 smoke generator; (**b**) Dantec Dual PIV laser; (**c**) High FPS camera.

The particles were blown into the mounting area of the ceiling lamp to ensure as much mixing of the supply air with the smoke particles as possible (Figure 14a) and were subsequently recorded in the red area above the operating table (Figure 14b). The volume flows of the ventilation system were identical to the boundary conditions of simulated variant 5.

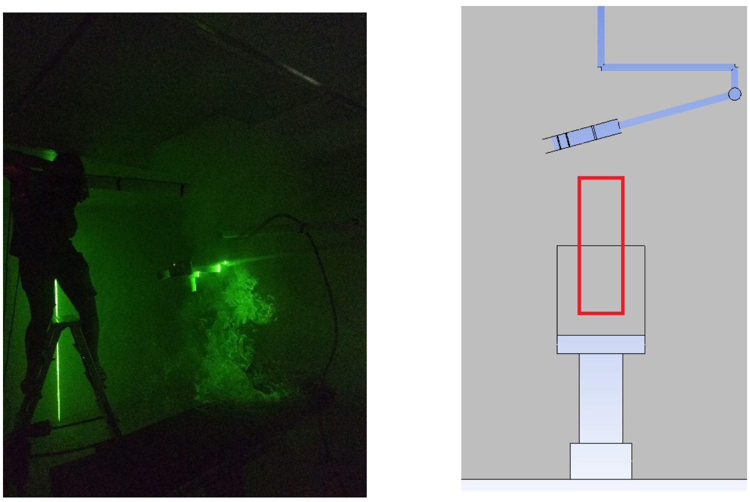

(**a**) (**b**)

Figure 14. Creation of airflow velocity profiles: (**a**) smoke generation to the measuring area; (**b**) area measured by the PIV method.

The velocity profile of the airflow generated in the measured area is shown in Figure 15a. The average air velocity in the monitored area was 0.14 m·s^{-1} (b). Figure 15b shows the same area in the CFD simulation for variant 5, using k–ω model 5 × 10^6 elements in the mesh, with inflation on the surface of the operating lamp. The sizes of the mesh elements ranged from 3–30 mm in order to achieve the lowest possible Y+ values in the viscous sublayer area; in addition, skewness quality and orthogonal quality were also monitored. It must be taken into account that airflow in the operating room is a dynamic process with slightly variable velocity profiles. Therefore, the velocity profile of the airflow in the simulation is not identical to the experimental measurement. While maintaining the same speed from LAFC, the speed similarity behind the operating light is high. The average air velocity in the monitored area was 0.13 m·s^{-1}. Figure 15c presents the use of the same number of elements in the mesh but is calculated by the k–ε model. For this turbulence model, the average airflow rate was only 0.04 m·s^{-1}. Quality control for the mesh was also performed by Chen et al. using half (2.5 × 10^6) and twice (10^7) the number of elements [46]. The differences in the results with twice the number of elements were negligible. A higher degree of similarity between experimental measurement and simulation was observed in flow model k-ω. The difference in the average airflow rate between the experimental measurement of the PIV method and the CFD simulation with turbulence model k-ω was approximately 7%.

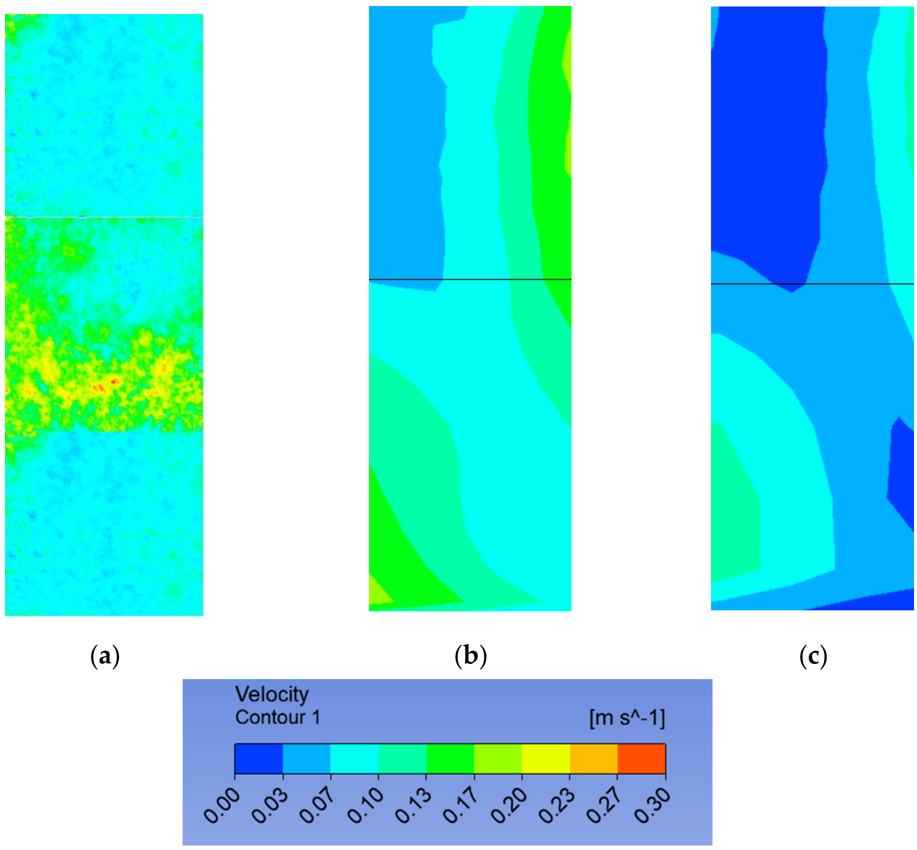

Figure 15. Comparison of air velocity profiles above the operating table: (**a**) measurement by the PIV method; (**b**) model k-ω; (**c**) model k-ε.

3. Discussion

The numerical results report that the highest concentration of particles in the volume of the V_{OT} was above the operating table for variant 3. It is believed that the nonlinear dependence of particle concentrations upon air velocity is due to two different mechanisms for eliminating particles from the clean zone area. The first mechanism works on the principle of diluting the concentration of particles in the air; the more filtered air is fed into the room, the lower is the concentration. This is the basic principle of cleanroom ventilation and is confirmed by the results of a study by Heidrich et al. [30] and Khoo et al. [2]. Our intention is to ensure good mixing throughout the room, which would lead to a uniformly low concentration of particles thereof [47]. The second option for achieving a low concentration of particles in the air is to eliminate unwanted turbulence in the clean zone area. An increased air flow rate is directly related to an increase in the kinetic energy of turbulence and the higher concentration of particles in the area above the operating table and instrument tables. The causative relationship between increased airflow rate and higher particle concentration is confirmed by Figures 7 and 11 (left) and the proportion of particles in the volume of $V_{IT\,2}$ for variants 1 and 5. In Figure 9 (right), the higher airflow rate above the operating table is visible and it confirms the dependence of increased particle concentration in the volume of V_{OT} for variant 3. These results show that lower flow rates reduce unwanted turbulence and the magnitude of velocity fluctuations, making the ventilation system more efficient at removing contaminants, leading to a reduction in ACH and a decrease in the operating costs of the system. This possibility, of reducing energy costs, is interesting when the locations and intensities of contaminant sources are well known [48].

The suitability of using CFD for airflow simulation and contaminants in a cleanroom is confirmed by several studies [19,32,47]. The SIMPLE algorithm was used in the study and the convergence criteria were set as 10^{-4}, with the exception of energy which was set as 10^{-6} [31]. Although some studies have used the k-ε model flow model for CFD simulations in combination with the re-normalized group (RNG), which is considered a more reliable method of simulating an indoor airflow pattern [49,50]. According to verification by the PIV method, the flow is more realistically expressed by the k-ω model. Lee et al. also list the PIV method as suitable for verifying airflow ventilation to evaluate CFD accuracy [51]. Model k-ω allows for more accurate near-wall treatment with an automatic switch from a wall function to a low Reynolds number formulation based on grid spacing, which demonstrates superior performance for wall-bounded and low Reynolds number flows. According to Menter and Pope, the k-ε model is only suitable for flow without separation and fully turbulent flow. The results of the k-ε models only showed good agreement for high Reynolds numbers and especially for the flow in the pipeline [52–54].

The significant effect of the airflow rate from LAFC may be noted based upon the economic operation of the cleanroom; a suitable heat-velocity microclimate, but also the number of particles emitted by staff clothing. Several studies have monitored the economic operation of a cleanroom due to its notoriously high energy consumption [2–5], looking for ways to reduce their operating costs, especially with regards to air supply and circulation [19] by modifying the position of distribution elements and pollution sources, or by reducing fan power (volume flow) [20]. As cleanroom operations continue to protect against off-site contamination, the overall savings are even more significant [21,55]. Reducing the flow rate from the distribution element below 0.2 $m \cdot s^{-1}$ has the effect of reducing the number of particles emitted from the clothing surfaces of the staff in the room [56]. According to Whyte [57,58] and Ljungqvist et al. [59] clothes are one of the most significant sources of particulate matter emissions in clean rooms. Moving a human body into the path of internal ventilation flows can also cause the penetration of particles [60]. Higher ACHs, which are often accompanied by a higher airflow rate via the distribution elements, create a feeling of thermal discomfort [32]. Thermal discomfort could cause doctors to commit errors in a clean room, which could, in turn, lead to health hazards. Most surgeons spend 85–90% of their time in cleanrooms [61], so the importance of choosing an appropriate flow rate for a cleanroom's ventilation is desirable.

In this work, methods and instruments were used that could have skewed the accuracy of the results. In the CFD model, the overpressure ventilation of the operating room was neglected and the same air volume flow through the supply and exhaust distribution elements were considered. In practice, 10–20% more air is supplied to the cleanroom to create a pressure cascade [62]. Guaranteed inaccuracy of up to 5% could also arise with the equipment used for the PIV method. The disadvantage to using ingested equipment is the small size of the monitored area during one measurement (approximately 200 × 200 mm). Therefore, only the most important areas between the lamp and the table were monitored. The three measurements were taken of the investigated area, with dimensions of 200 × 600 mm. The temperature of the supplied air and the speed of the airflow in the investigated area have a certain influence on the nature of the flow. The experimental measurement was similar to the simulation, in that it was solved as an isothermal problem. To ensure a temperature-neutral environment, thermal insulation with a thickness of 250–400 mm was used on the perimeter walls of the laboratory. The nature of the flow and changes in the velocity profiles could be influenced by the smoke generator for the PIV device. The smoke generator was placed close to the distribution element above the operating light and particles were flowing with a velocity in the range of 1.0–2.5 $m \cdot s^{-1}$ Figure 14a.

4. Conclusions

This work deals with the effects of air velocity, supplied to the operating room via LAFC (in the range of 0.15–0.25 $m \cdot s^{-1}$) and on the change in particle concentration of 0.5 μm. A numerical simulation, created with Ansys Fluent software, was used to evaluate the changes in particle concentration. The concentration differences between the worst (1.51%) and most efficient (0.70%) particle removal variants represent an improvement of approximately 54%. The numerical results indicate that lower operating speeds of the ventilation system (0.15–0.175 $m \cdot s^{-1}$) are more advantageous in terms of particle removal efficiency in the operating table area and also decrease costs due to lower ACH. The area representing the instrument tables was most significantly affected by the higher airflow rate and this resulted in a higher concentration of particles therein. From these airflow profiles, the relationship between the increased particle concentrations in the air and a local increase in air velocity was confirmed. During the verification of the CFD simulation of the airflow between the operating table and the luminaire, the k-ω flow model was verified as more appropriate, with an approximate inaccuracy of 7%.

Author Contributions: Conceptualization, P.M.; methodology, P.M.; validation, P.M. and D.H.; formal analysis, R.N.; investigation, D.H.; resources, A.K.; data curation, R.N., Z.K., P.H. and N.Č.K.; writing—original draft preparation, P.M.; writing—review and editing, R.N.; supervision, A.K.; project administration, P.M. and A.K.; funding acquisition, P.M. and A.K. All authors have read and agreed to the published version of the manuscript.

Funding: This research was funded by project APVV PP-COVID-20-0113 "Creation of clean operating rooms in order to reduce the risk of transmission and spread of COVID-19 virus and other viruses and bacteria, with ensured decontamination of exhaust air from the clean room", and project of Operational Programme Integrated Infrastructure: Independent research and development of technological kits based on wearable electronics products, such as tools for raising hygienic standards in a society exposed to the COVID- 19 disease, ITMS2014+ code 313011ASK8. The project is co-funded by the European Regional Development Fund.

Institutional Review Board Statement: Not applicable.

Informed Consent Statement: Not applicable.

Data Availability Statement: Data available in a publicly accessible repository.

Conflicts of Interest: The funders had no role in the design of the study; in the collection, analyses, or interpretation of data; in the writing of the manuscript, or in the decision to publish the results. The authors declare no conflict of interest.

References

1. EU. *ANNEX 1 Manufacture of Sterile Medicinal Products*; No. November; European Commission: Brussels, Belgium, 2008; Volume 4, pp. 1–16.
2. Khoo, C.Y.; Lee, C.-C.; Hu, S.-C. An experimental study on the influences of air change rate and free area ratio of raised-floor on cleanroom particle concentrations. *Build. Environ.* **2012**, *48*, 84–88. [CrossRef]

3. Fedotov, A. Saving energy in cleanrooms. *Cleanroom Technol.* **2014**, *22*, 14–18.
4. Tschudi, W.; Xu, T. Cleanroom energy benchmarking results. *ASHRAE Trans.* **2002**, *109*, 733–739.
5. Kircher, K.; Shi, X.; Patil, S.; Zhang, K.M. Cleanroom energy efficiency strategies: Modeling and simulation. *Energy Build.* **2010**, *42*, 282–289. [CrossRef]
6. *ISO 14644-1*; Cleanrooms and Associated Controlled Environments—Part 1: Classification of Air Cleanliness; ISO: Geneva, Switzerland, 2015.
7. Department of Health. Making Best Use of Medicines, Report, UK. 2011. p. 16. Available online: https://assets.publishing.service.gov.uk/government/uploads/system/uploads/attachment_data/file/216705/dh_129216.pdf (accessed on 22 October 2021).
8. Birks, S. Opinion ACRs—Time for change? *Cosmetics Business*. 2013. Available online: https://www.cosmeticsbusiness.com/news/article_page/Opinion_ACRs__Time_for_change/89740 (accessed on 27 October 2021).
9. Hu, S.-C.; Chuah, Y. Power consumption of semiconductor fabs in Taiwan. *Energy* **2003**, *28*, 895–907. [CrossRef]
10. Hu, S.; Chuah, Y.; Yen, M. Design and evaluation of a minienvironment for semiconductor manufacture processes. *Build. Environ.* **2002**, *37*, 201–208. [CrossRef]
11. Nada, S.; Elfeky, K. Experimental investigations of thermal managements solutions in data centers buildings for different arrangements of cold aisles containments. *J. Build. Eng.* **2016**, *5*, 41–49. [CrossRef]
12. Sun, W.; Mitchell, J.; Flyzik, K.; Hu, S.C.; Liu, J.; Vijayakumar, R.; Fukuda, H. Development of cleanroom required airflow rate model based on establishment of theoretical basis and lab validation. *ASHRAE Trans.* **2010**, *116*, 87–97.
13. Chuah, Y.; Tsai, C.-H.; Hu, S. Simultaneous control of particle contamination and VOC pollution under different operating conditions of a mini-environment that contains a coating process. *Build. Environ.* **2000**, *35*, 91–99. [CrossRef]
14. Murakami, S.; Kato, S.; Nagano, S.; Tanaka, Y. Diffusion characteristics of airborne particles with gravitational settling in a convection-dominant indoor flow field. *ASHRAE Trans.* **1992**, *98*, 82–97.
15. Zhao, B.; Wu, J. Numerical Investigation of Particle Diffusion in a Clean Room. *Indoor Built Environ.* **2005**, *14*, 469–479. [CrossRef]
16. Sartor, D.; Lowell, C.; Blumstein, C. *Cleanrooms and Laboratories for High Tech Industries, Final Report*; California Energy Commission: Sacramento, CA, USA, 1999.
17. Mills, E.; Bell, G.; Sartor, D.; Chen, A.; Avery, D.; Siminovitch, M.; Greenberg, S.; Marton, G.; de Almeida, A.; Lock, L.E. *Energy Efficiency in California Laboratory-Type Facilities*; LBNL-39061; Lawrence Berkeley National Laboratory: Berkeley, CA, USA, 1996.
18. Tschudi, W.; Sartor, D.; Mills, E.; Xu, T. *High-Performance Laboratories and Cleanrooms*; LBNL-50599; Lawrence Berkeley National Laboratory: Berkeley, CA, USA, 2002.
19. Loomans, M.G.L.C.; Molenaar, P.C.A.; Kort, H.S.M.; Joosten, P.H. Energy demand reduction in pharmaceutical cleanrooms through optimization of ventilation. *Energy Build.* **2019**, *202*, 109346. [CrossRef]
20. Tschudi, W.; Mills, E.; Tenfang, X.; Rumsey, P. Measuring and managing cleanroom energy use. *Heat. Pip. Air Cond. Eng.* **2005**, *77*, 29–35.
21. Faulkner, D.; Fisk, W.J.; Walton, J.T. Energy savings in cleanrooms from demand-controlled filtration. *Indoor Environ.* **1996**, *39*, 21–27. [CrossRef]
22. Faulkner, D.; DiBartolomeo, D.; Wang, D. *Demand Controlled Filtration in an Industrial Cleanroom*; LBNL-63420; Lawrence Berkeley National Laboratory: Berkeley, CA, USA, 2007; p. 11.
23. Tschudi, W.; Faulkner, D.; Hebert, A. Energy efficiency strategies for cleanrooms without compromising environmental conditions, Part 2. *ASHRAE Trans.* **2005**, *111*, 637–645.
24. Sharp, G.P. Demand-based control for lab ventilation. *Cleanroom Technol.* **2013**, *21*, 29–33.
25. Hu, S.-C.; Shiue, A. Validation and application of the personnel factor for the garment used in cleanrooms. *Build. Environ.* **2016**, *97*, 88–95. [CrossRef]
26. Xu, T. Efficient Airflow Design for Cleanrooms Improves Business Bottom Lines. In Proceedings of the Efficient Airflow Design for Cleanrooms Improves Business Bottom Lines, Berkeley, CA, USA, 5 January 2003.
27. *U.S. Federal Standard FS209*; Clean Room and Work Station Requirements, Controlled Environment; General Services Administration: Washington, DC, USA, 1973.
28. IEST-RP-CC012: CONSIDERATIONS IN CLEANROOM DESIGN. Available online: https://www.iest.org/Standards-RPs/Recommended-Practices/IEST-RP-CC012 (accessed on 4 January 2022).
29. *ISO 14644-4*; Cleanrooms and Associated Controlled Environments—Part 4: Design, Construction and Start-Up; ISO: Geneva, Switzerland, 2004.
30. Heidrich, T.; Alimi, A.; Grothues, L.; Hesselbach, J.; Wünsch, O. Cross-flowing displacement ventilation system for conveyor belts in the food industry. *Energy Build.* **2018**, *179*, 213–222. [CrossRef]
31. Zhao, F.-Y.; Cheng, J.; Liu, B.; Huang, Z.-R.; Li, X. Indoor airflow and pollutant spread inside the cleanroom with micro-porous supplying panel and different ventilation schemes: Analytical, numerical and experimental investigations. *J. Build. Eng.* **2020**, *31*, 101405. [CrossRef]
32. Zhao, F.-Y.; Cheng, J.; Liu, B.; Huang, Z.-R.; Zhang, Y.-J.; Li, X. Regional flow motion and heat energy balance analysis of a 10,000 class pharmaceutical cleanroom with secondary return air conditioning system. *Int. J. Refrig.* **2021**, *129*, 237–249. [CrossRef]
33. Brown, W.K.; Lynn, C.A. Fundamental clean room concepts. *ASHRAE Trans.* **1986**, *92*, 272–287.
34. Jaisinghani, R.A. Air handling considerations for cleanrooms. In Proceedings of the InterPhex Conference, Philadelphia, PA, USA, 20–22 March 2001; p. 15.

35. Kozicki, M.; Robinson, P.; Hoenig, S.A. *Cleanrooms, Facilities and Practices*; Van Nostrand Reinhold: New York, NY, USA, 1991; ISBN 9401179514.
36. Morrison, P.W. *Environmental Control in Electronic Manufacturing*; Van Nostrand Reinhold: New York, NY, USA, 1973; ISBN 0442255640.
37. Villafruela, J.M.; Castro, F.; José, J.F.S.; Saint-Martin, J. Comparison of air change efficiency, contaminant removal effectiveness and infection risk as IAQ indices in isolation rooms. *Energy Build.* **2013**, *57*, 210–219. [CrossRef]
38. Häkkinen, T.; Kuittinen, M.; Ruuska, A.; Jung, N. Reducing embodied carbon during the design process of buildings. *J. Build. Eng.* **2015**, *4*, 1–13. [CrossRef]
39. Zhang, R.; Tu, G.B.; Ling, J.H. Study on biological contaminant control strategies under different ventilation models in hospital operating room. *Build. Environ.* **2008**, *43*, 793–803.
40. Tao, Y.; Gou, Z.; Yu, Z.; Fu, J.; Chen, X. The challenge of creating age-friendly indoor environments in a high-density city: Case study of Hong Kong's care and attention homes. *J. Build. Eng.* **2020**, *30*, 101280. [CrossRef]
41. Noh, K.C.; Kim, H.S.; Oh, M.D. Study on contamination control in a minienvironment inside clean room for yield enhancement based on particle concentration measurement and airflow CFD simulation. *Build. Environ.* **2010**, *45*, 825–831. [CrossRef]
42. Xu, T. Characterization of minienvironments in a clean room: Design characteristics and environmental performance. *Build. Environ.* **2007**, *42*, 2993–3000. [CrossRef]
43. Cheng, M.; Liu, G.; Cai, K.W.; Lee, E. Approaches for improving airflow uniformity in unidirectional flow cleanrooms. *Build. Environ.* **1998**, *34*, 275–284. [CrossRef]
44. Cleanroom Technology. Study into Human Particle Shedding. 2011. Available online: https://www.cleanroomtechnology.com/news/article_page/Study_into_human_particle_shedding/62768 (accessed on 4 August 2021).
45. Kim, C.; Cho, K.; Pui, D.Y.H. Investigation of Airborne Molecular Contamination in Cleanroom Air Environment through Portable Soft X-Ray Radiolysis Detector. *Appl. Sci.* **2020**, *10*, 978. [CrossRef]
46. Chen, Q.; Srebric, J. A Procedure for Verification, Validation, and Reporting of Indoor Environment CFD Analyses. *HVAC&R Res.* **2002**, *8*, 201–216. [CrossRef]
47. Naosungeon, J.; Thongsri, J. Simulation of Airflow in a Cleanroom to Solve Contamination Problem in an HDD Production Line. *Int. J. Mech. Eng. Robot. Res.* **2018**, *7*, 41–45.
48. Novoselac, A.; Srebric, J. Comparison of air exchange efficiency and contaminant removal effectiveness as IAQ indices. *ASHRAE Trans.* **2003**, *109*, 339–349.
49. Li, X.P.; Niu, J.L.; Gao, N.P. Spatial distribution of human respiratory droplet residuals and exposure risk for the co-occupant under different ventilation methods. *HVAC&R Res.* **2011**, *17*, 432–455.
50. Zhang, L.; Li, Y. Dispersion of coughed droplets in a fully-occupied high-speed rail cabin. *Build. Environ.* **2012**, *47*, 58–66. [CrossRef]
51. Lee, I.; Lee, S.; Kim, G.; Sung, J.; Sung, S.; Yoon, Y. Piv verification of greenhouse ventilation air flows to evaluate cfd accuracy. *Trans. ASAE* **2005**, *48*, 2277–2288. [CrossRef]
52. Menter, F.R. Zonal Two Equation k- ω Turbulence Models for Aerodynamic Flows. In Proceedings of the 24th Fluid Dynamics Conference, Orlando, FL, USA, 6–9 July 1993. AIAA Paper 93-2906.
53. Menter, F.R. Two-equation eddy-viscosity turbulence models for engineering applications. *AIAA J.* **1994**, *32*, 1598–1605. [CrossRef]
54. Pope, S.B. *Turbulent Flows*; Cambridge University Press: Cambridge, UK, 2000; ISBN 978-0521598866.
55. Energy management. Available online: https://www.sciencedirect.com/science/article/pii/S0378778819308102 (accessed on 20 January 2022).
56. Foarde, K.; Hill, L.; Hanley, J. Measurement and Detection of Cleanroom Fabric Barrier and Shedding Properties. *J. IEST* **2000**, *43*, 26–31. [CrossRef]
57. Whyte, W.; Bailey, P.V. Reduction of microbial dispersion by clothing. *PDA J. Pharm. Sci. Technol.* **1985**, *39*, 51–61.
58. Whyte, W.; Bailey, P. Particle Dispersion in Relation to Clothing. *J. IEST* **1989**, *32*, 43–49. [CrossRef]
59. Ljungqvist, B.; Reinmüller, B. *Cleanroom Clothing Systems, Practical Safety Ventilation in Pharmaceutical and Biotech Cleanrooms*; Parenteral Drug Association: Bethesda, MD, USA, 2006; pp. 57–76.
60. Vokac, Z.; Køpke, V.; Keül, P. Assessment and Analysis of the Bellows Ventilation of Clothing. *Text. Res. J.* **1973**, *43*, 474–482. [CrossRef]
61. Klepeis, N.E.; Nelson, W.C.; Ott, W.R.; Robinson, J.P.; Tsang, A.M.; Switzer, P.; Behar, J.V.; Hern, S.C.; Engelmann, W.H. The National Human Activity Pattern Survey (NHAPS): A resource for assessing exposure to environmental pollutants. *J. Expo. Sci. Environ. Epidemiol.* **2001**, *11*, 231–252. [CrossRef] [PubMed]
62. Whyte, W. *Cleanroom Design*, 2nd ed.; John Wiley & Sons Ltd.: Choichester, UK, 1999; ISBN 0-471-94294-9.